Supplementary materials

Two-dimensional heterostructures of AuSe/SnS for the photocatalytic hydrogen evolution reaction with Z-scheme

Qi-Kang Yin, Chuan-Lu Yang *, Mei-Shan Wang, Xiao-Guang Ma

School of Physics and Optoelectronic Engineering, Ludong University, Yantai 264025, China

1. Additional materials for the structural and electronic properties of the AuSe and SnS monolayers as well as the AuSe/SnS heterostructure

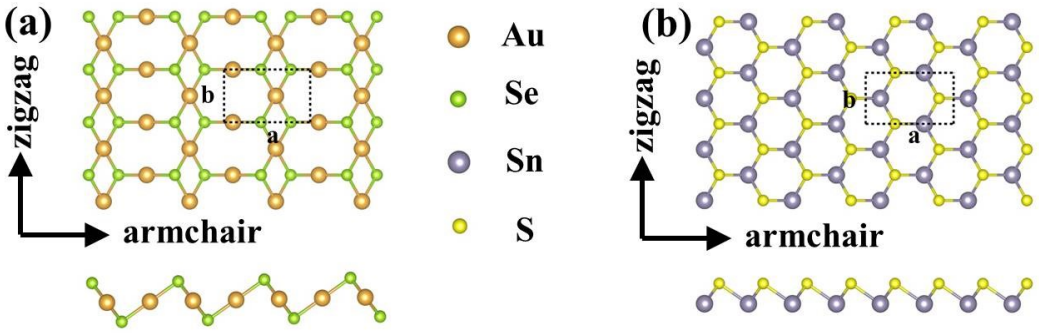

Fig.S1. The top and side views for the supercell of the AuSe and SnS monolayers, respectively.

*Corresponding author. *E-mail address:* ycl@ldu.edu.cn. (C.L. Yang).

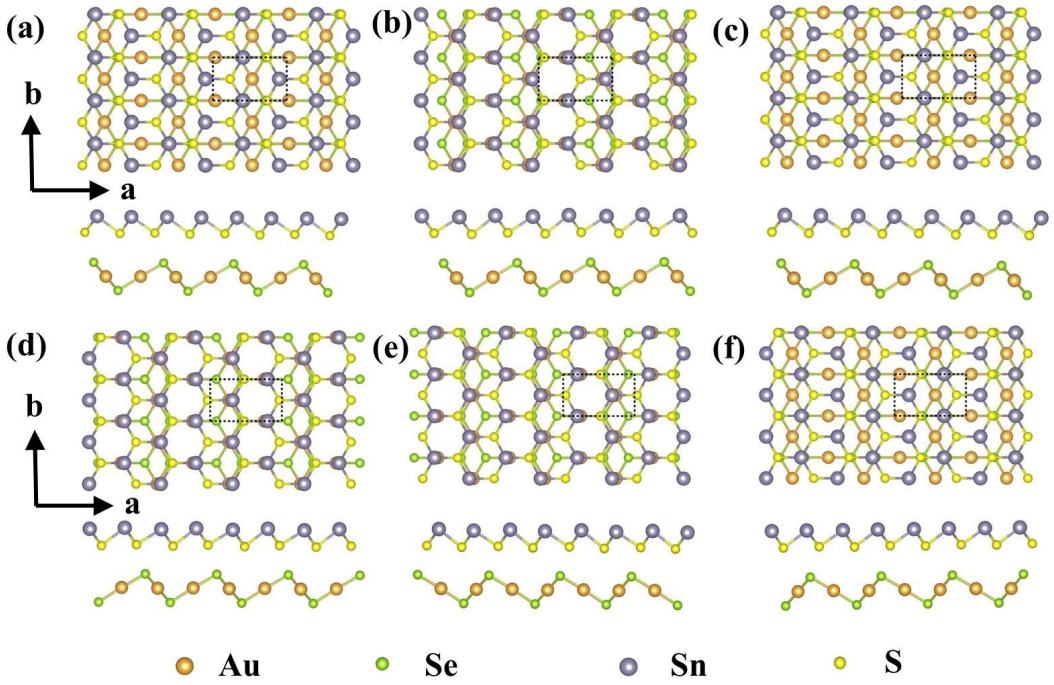

Fig.S2. The top and side views of the additional six configurations of the AuSe/SnS heterostructure. (a) ASx, (b) ASy, (c) AxSx, (d) AxSy, (e) AySx, and (f) AySy, respectively.

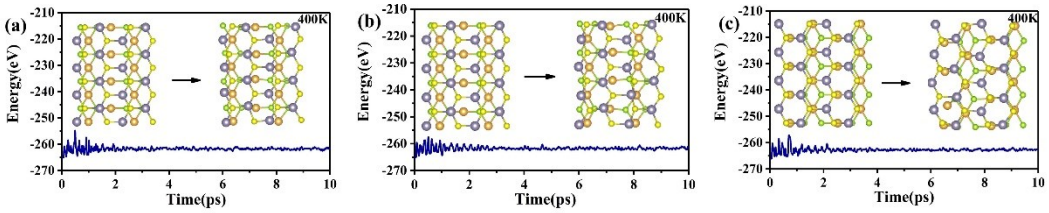

Fig.S3. Total energy fluctuations during AIMD simulations for the AuSe/SnS heterostructures at 400K, the snapshots of the structures at 10 ps are also included. (a), (b) and (c) represent AS, AxS, and AyS configurations, respectively.

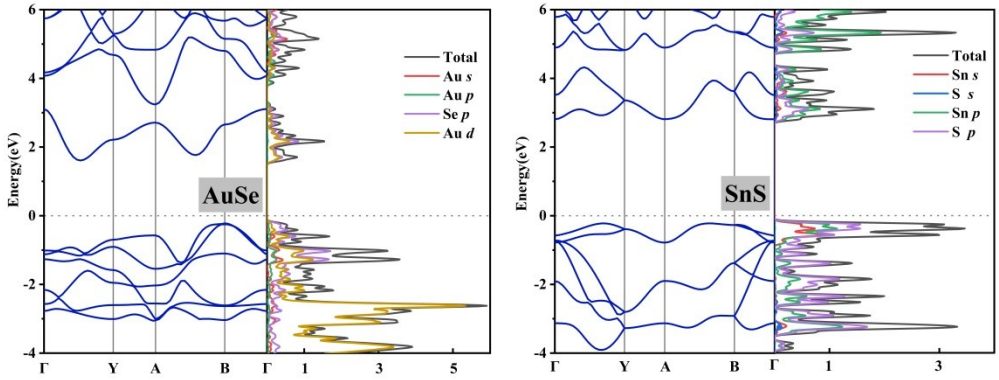

Fig.S4. The band structures and density of state for the AuSe and SnS monolayers by HSE06. (a) AuSe, (b) SnS.

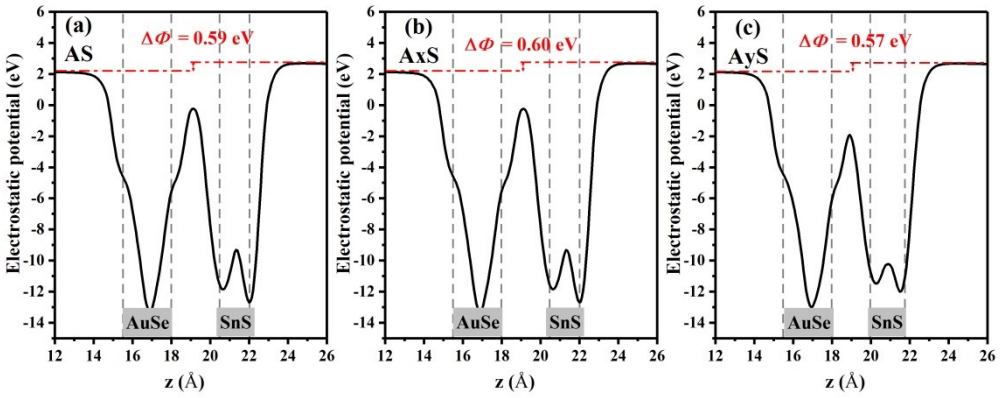

Fig.S5. The electrostatic potentials and the difference of the vacuum energy levels ($\Delta\Phi$) for the AS, AxS, and AyS configurations of the AuSe/SnS heterostructure.

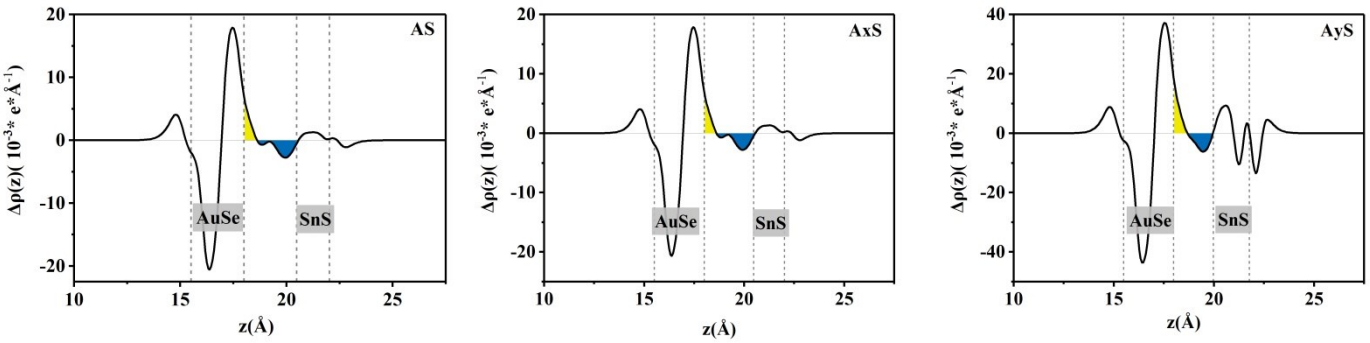

Fig.S6. The curve of plane-integrated electron density difference along with the *z*-direction for the AS, AxS, and AyS configurations. Dotted lines mark the positions of the two monolayers.

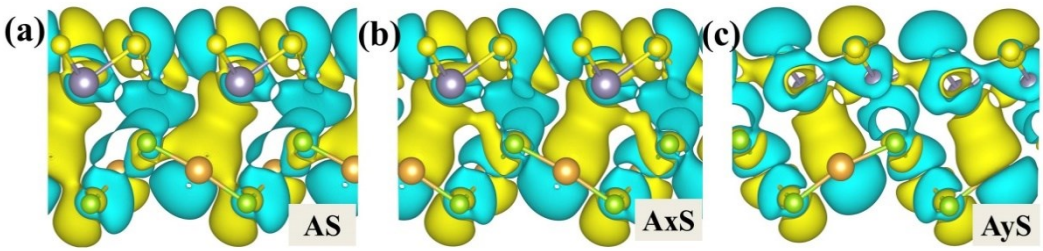

Fig.S7. The 3D isosurface of the charge density difference. (a) AS, (b) AxS, and (c) AyS configurations. The yellow and blue regions represent electron accumulation and depletion, respectively. The isosurface value is 0.0007e/Å^3.

2. The details of the calculation method and results of solar-to-hydrogen（STH）

According to the calculation methodology of STH efficiency (η_{STH}) proposed by Fu *et al*. [1] Where η_{abs} and η_{cu} are the efficiency of light absorption and carrier utilization, respectively. Where $P(\hbar\omega)$ is the expression for the AM 1.5G solar energy

flux by the photon energy $h\omega$, band gaps E_g (HSE) is the bandgap of layered materials. Calculated the over-potential for hydrogen evolution reaction $\chi(H_2)$, and the overpotential for oxygen evolution reaction $\chi(O_2)$ of strained AuSe/SnS heterostructure. Where ΔV is the potential difference of 1.23 eV for water splitting, and E is the energy of photons that can actually be utilized for water splitting. Where $\Delta\Phi$ is the vacuum level difference on the two surfaces of these 2D heterostructures, the energy conversion efficiency of light absorption is defined as η_{abs}, the efficiency of carrier utilization is defined as η_{cu}, STH efficiency is defined as η_{STH}, and corrected STH efficiency of photocatalytic water splitting is defined as η'_{STH}.

$$\eta_{STH} = \eta_{abs} \times \eta_{cu} \tag{1}$$

$$\eta_{abs} = \frac{\int_{E_g}^{\infty} P(h\omega)d(h\omega)}{\int_{0}^{\infty} P(h\omega)d(h\omega)}$$

(2)

$$\eta_{cu} = \frac{\Delta V \int_{E}^{\infty} \frac{P(h\omega)}{h\omega} d(h\omega)}{\int_{E_g}^{\infty} P(h\omega)d(h\omega)}$$

(3)

$$E = \begin{cases} E_g, \left(\chi(H_2) \geq 0.2, \chi(O_2) \geq 0.6\right) \\ E_g + 0.2 - \chi(H_2), \left(\chi(H_2) < 0.2, \chi(O_2) \geq 0.6\right) \\ E_g + 0.6 - \chi(O_2), \left(\chi(H_2) \geq 0.2, \chi(O_2) < 0.6\right) \\ E_g + 0.8 - \chi(H_2) - \chi(O_2), \left(\chi(H_2) < 0.2, \chi(O_2) < 0.6\right) \end{cases} \quad (4)$$

$$\eta_{STH}^{'} = \eta_{STH} \times \frac{\int_0^{\infty} P(h\omega)d(h\omega)}{\int_0^{\infty} P(h\omega)d(h\omega) + \Delta\Phi \int_0^{\infty} \frac{P(h\omega)}{h\omega} d(h\omega)} \quad (5)$$

The following tables are the results obtained by considering the vacuum energy levels of hydrogen evolution reaction (HER) and oxidation evolution reaction (OER), only the vacuum energy levels on the OER side and only the vacuum energy levels on the HER side.

Table S1. $\eta_{STH}^{'}$ of the AS configuration based on I-V_{vac}.

Configuration(AS)	$\chi(H_2)(eV)$	$\chi(O_2)(eV)$	E_g(HSE)	$\Delta\Phi$(eV)	η_{abs}(%)	η_{cu}(%)	η_{STH}(%)	$\eta_{STH}^{'}$(%)
-4%	0.33	1.00	2.19	0.10	29.91	45.78	13.67	13.52
-3%	0.23	1.03	2.10	0.10	33.51	46.96	15.74	15.56
-2%	0.22	1.8	2.06	0.11	35.28	47.57	16.79	16.54
-1%	0.21	1.16	2.03	0.12	36.49	47.99	17.51	17.22
0	0.20	1.18	2.00	0.20	37.82	48.44	18.32	17.79
1%	0.19	1.29	1.97	0.18	39.26	48.26	18.95	18.43
2%	0.18	1.35	1.94	0.20	40.72	48.30	19.67	19.04

3%	0.17	1.40	1.90	0.23	42.89	47.59	20.41	19.62
4%	0.16	1.41	1.82	0.25	46.57	48.63	22.52	21.48

Table S2. $\eta_{STH}^{'}$ of the AxS configuration based on I-V_{vac}.

Configuration(AxS)	$\chi(H_2)(eV)$	$\chi(O_2)(eV)$	E_g(HSE)	$\Delta\Phi$(eV)	$\eta_{abs}(\%)$	$\eta_{cu}(\%)$	$\eta_{STH}(\%)$	$\eta_{STH}^{'}(\%)$
-4%	0.32	1.01	2.25	0.12	27.63	44.90	12.41	12.26
-3%	0.23	1.05	2.21	0.13	29.00	45.38	13.16	12.98
-2%	0.21	1.13	2.19	0.13	29.77	45.65	13.59	13.40
-1%	0.21	1.18	2.17	0.15	30.81	46.02	14.1	13.94
0	0.22	1.26	2.13	0.15	32.01	46.44	14.87	14.60
1%	0.23	1.30	2.10	0.18	33.51	46.96	15.74	15.38
2%	0.24	1.35	2.04	0.17	36.19	47.88	17.33	16.92
3%	0.24	1.36	1.96	0.18	39.84	49.14	19.58	19.03
4%	0.26	1.36	1.88	0.19	43.56	50.42	21.96	21.24

Table S3. $\eta_{STH}^{'}$ of the AyS configuration based on I-V_{vac}.

Configuration(AyS)	$\chi(H_2)(eV)$	$\chi(O_2)(eV)$	E_g(HSE)	$\Delta\Phi$(eV)	$\eta_{abs}(\%)$	$\eta_{cu}(\%)$	$\eta_{STH}(\%)$	$\eta_{STH}^{'}(\%)$
-4%	0.18	1.24	2.27	0.08	26.71	43.04	11.50	11.41
-3%	0.08	1.30	2.24	0.09	27.94	36.82	10.29	10.19
-2%	–	1.36	2.21	0.10	–	–	–	–
-1%	–	1.39	2.14	0.10	–	–	–	–
0	–	1.40	2.06	0.12	–	–	–	–
1%	–	1.41	1.98	0.12	–	–	–	–
2%	–	1.42	1.90	0.12	–	–	–	–

3%	–	1.43	1.83	0.13	–	–	–	–
4%	–	1.44	1.76	0.13	–	–	–	–

Table S4. $\eta_{STH}^{'}$ of the AS configuration based on II-V_{vac}.

Configuration(AS)	$\chi(H_2)(eV)$	$\chi(O_2)(eV)$	E_g(HSE)	$\Delta\Phi$(eV)	$\eta_{abs}(\%)$	$\eta_{cu}(\%)$	$\eta_{STH}(\%)$	$\eta_{STH}^{'}(\%)$
-4%	0.43	1.00	2.19	0	29.91	45.70	13.67	13.67
-3%	0.32	1.02	2.10	0	33.51	46.96	15.74	15.74
-2%	0.33	1.08	2.06	0	35.28	47.57	16.79	16.79
-1%	0.33	1.16	2.03	0	36.49	47.99	17.51	17.51
0	0.40	1.18	2.00	0	37.82	48.44	18.32	18.32
1%	0.37	1.29	1.97	0	39.26	48.94	19.22	19.22
2%	0.38	1.35	1.94	0	40.72	49.44	20.13	20.13
3%	0.40	1.40	1.89	0	42.89	50.19	21.52	21.52
4%	0.41	1.41	1.82	0	46.57	51.46	23.96	23.96

Table S5. $\eta_{STH}^{'}$ of the AxS configuration based on II-V_{vac}.

Configuration(AxS)	$\chi(H_2)(eV)$	$\chi(O_2)(eV)$	E_g(HSE)	$\Delta\Phi$(eV)	$\eta_{abs}(\%)$	$\eta_{cu}(\%)$	$\eta_{STH}(\%)$	$\eta_{STH}^{'}(\%)$
-4%	0.44	1.01	2.25	0	27.63	44.90	12.41	12.41
-3%	0.36	1.05	2.21	0	29.00	45.38	13.16	13.16
-2%	0.34	1.13	2.19	0	29.77	45.65	13.59	13.59
-1%	0.36	1.18	2.17	0	30.81	46.02	14.18	14.18
0	0.38	1.26	2.13	0	32.01	46.44	14.87	14.87
1%	0.41	1.30	2.10	0	33.51	46.96	15.74	15.74
2%	0.41	1.35	2.04	0	36.19	47.88	17.33	17.33

3%	0.42	1.36	1.96	0	39.84	49.14	19.58	19.58
4%	0.45	1.36	1.88	0	43.56	50.42	21.96	21.96

Table S6. $\eta_{STH}^{'}$ of the AyS configuration based on II-V_{vac}.

Configuration(AyS)	$\chi(H_2)(eV)$	$\chi(O_2)(eV)$	E_{g}(HSE)	$\Delta\Phi$(eV)	$\eta_{abs}(\%)$	$\eta_{cu}(\%)$	$\eta_{STH}(\%)$	$\eta_{STH}^{'}(\%)$
-4%	0.26	-1.24	2.27	0	26.71	44.57	11.90	11.90
-3%	0.17	-1.30	2.24	0	27.94	42.90	11.99	11.99
-2%	0.09	-1.36	2.21	0	29.31	37.83	11.09	11.09
-1%	0.08	-1.39	2.14	0	31.86	37.89	12.07	12.07
0	0.07	-1.40	2.06	0	35.14	38.90	13.67	13.67
1%	0.06	-1.41	1.98	0	38.69	39.35	15.22	15.22
2%	0.05	-1.42	1.90	0	42.31	39.67	16.79	16.79
3%	0.03	-1.43	1.83	0	46.14	40.41	18.50	18.50
4%	0.02	-1.44	1.76	0	49.83	40.78	20.32	20.32

Table S7. $\eta_{STH}^{'}$ of the AS configuration based on III-V_{vac}.

Configuration(AS)	$\chi(H_2)(eV)$	$\chi(O_2)(eV)$	E_{g}(HSE)	$\Delta\Phi$(eV)	$\eta_{abs}(\%)$	$\eta_{cu}(\%)$	$\eta_{STH}(\%)$	$\eta_{STH}^{'}(\%)$
-4%	0.33	1.10	2.19	0	29.91	45.70	13.67	13.67
-3%	0.23	1.11	2.10	0	33.51	46.96	15.74	15.74
-2%	0.22	1.19	2.06	0	35.28	47.57	16.79	16.79
-1%	0.21	1.28	2.03	0	36.49	47.99	17.51	17.51
0	0.20	1.38	2.00	0	37.82	48.44	18.32	18.32
1%	0.19	1.47	1.97	0	39.26	48.26	18.95	18.95
2%	0.18	1.55	1.94	0	40.72	48.30	19.67	19.67

3%	0.17	1.63	1.89	0	42.89	47.59	20.41	20.41
4%	0.16	1.66	1.82	0	46.57	54.46	23.96	23.96

Table S8. $\eta_{STH}^{'}$ of the AxS configuration based on III-V_{vac}.

Configuration(AxS)	$\chi(H_2)(eV)$	$\chi(O_2)(eV)$	E_{g}(HSE)	$\Delta\Phi$(eV)	$\eta_{abs}(\%)$	$\eta_{cu}(\%)$	$\eta_{STH}(\%)$	$\eta_{STH}^{'}(\%)$
-4%	0.32	1.13	2.25	0	27.63	44.90	12.41	12.41
-3%	0.23	1.18	2.21	0	29.00	45.38	13.16	13.16
-2%	0.21	1.26	2.19	0	29.77	45.65	13.59	13.59
-1%	0.21	1.33	2.17	0	30.81	46.02	14.18	14.18
0	0.23	1.41	2.13	0	32.01	46.44	14.87	14.87
1%	0.23	1.48	2.10	0	33.51	46.96	15.74	15.74
2%	0.24	1.52	2.04	0	36.19	47.88	17.33	17.33
3%	0.24	1.54	1.96	0	39.84	49.14	19.58	19.58
4%	0.26	1.55	1.88	0	43.56	50.42	21.96	21.96

Table S9. $\eta_{STH}^{'}$ of the AyS configuration based on III-V_{vac}.

Configuration(AyS)	$\chi(H_2)(eV)$	$\chi(O_2)(eV)$	E_{g}(HSE)	$\Delta\Phi$(eV)	$\eta_{abs}(\%)$	$\eta_{cu}(\%)$	$\eta_{STH}(\%)$	$\eta_{STH}^{'}(\%)$
-4%	0.18	1.32	2.27	0	26.71	43.04	11.50	11.50
-3%	0.08	1.39	2.24	0	27.94	36.82	10.29	10.29
-2%	–	1.46	2.21	0	–	–	–	–
-1%	–	1.49	2.14	0	–	–	–	–
0	–	1.52	2.06	0	–	–	–	–
1%	–	1.53	1.98	0	–	–	–	–
2%	–	1.54	1.90	0	–	–	–	–

3%	–	1.56	1.83	0	–	–	–	–
4%	–	1.57	1.76	0	–	–	–	–

3. Detail calculations and results for the effective mass and mobility of carriers

The carrier mobility can be calculated by employing the deformation potential (DP) theory [2]:

$$\mu = \frac{2e\hbar^3 C}{3K_B T|m^*|^2 E_d^2} \quad (6)$$

Here, T is the temperature; e represents electronic charge, $\hbar$,K_B means the reduced Planck constant and Boltzmann constant. C is elastic modulus with the formula of $C=\frac{1}{S_0}\frac{\partial^2 E}{\partial \varepsilon^2}$. Where E is the total energy obtained after structural deformation and ε is the uniaxial strain along with the armchair or zigzag direction of the rectangle cell, while S_0 is the area of the monolayer. E_d is DP constant and calculated by $E_d = \frac{\partial E_{edge}}{\partial \varepsilon}$, E_{edge} is the energy of band edge under uniaxial strain. m^* is effective mass, which can be obtained with $\frac{1}{m^*} = \frac{1}{\hbar^2}\frac{d^2E(k)}{dk^2}$, where k represents wave vector and $E(k)$ is the energy that corresponds to k. all the calculations are completed with HSE06.

Table S10. The carrier mobilities of the AuSe monolayer and SnS monolayer.

monolayer	Carrier type	m_{arm}^* (m_0)	m_{zig}^* (m_0)	C_{arm} (N/m)	C_{zig} (N/m)	E_d^{arm} (eV)	E_d^{zig} (eV)	μ_{arm} (cm^2/ V.s)	μ_{zig} (cm^2/ V.s)
AuSe	electron	1.96	0.76	59.39	74.26	1.28	4.17	1.34×10^2	1.04×10^2
	hole	0.55	0.48	59.39	74.26	0.86	5.38	3.72×10^4	1.59×10^2
SnS	electron	0.85	0.45	43.86	43.68	1.50	4.24	3.84×10^2	1.71×10^2
	hole	2.94	1.31	43.86	43.68	0.28	1.94	9.18×10^2	9.66×10^1

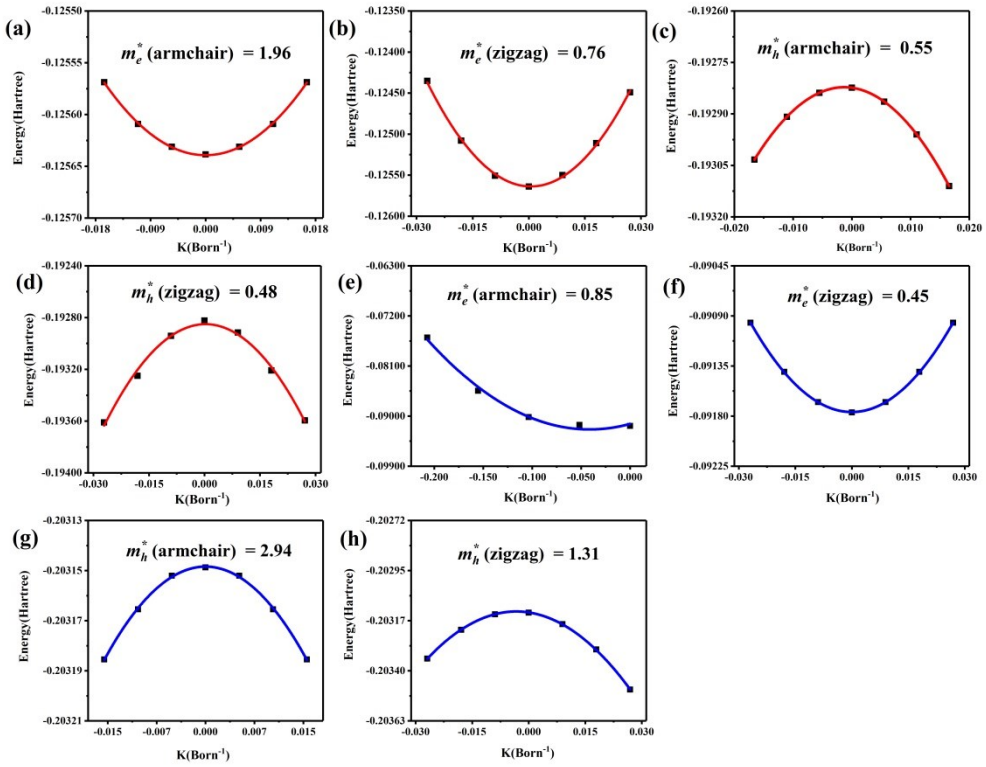

Fig.S8. The effective masses of electrons (m_e*) and holes (m_h*). Red lines represent AuSe, and blue lines represent SnS.

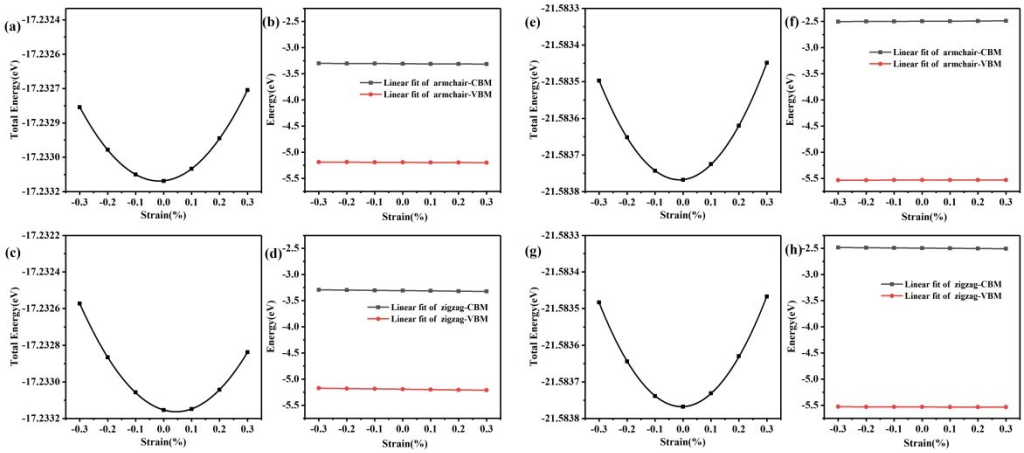

Fig.S9. The relationship between total energy and the applied strain and the fitted details for the DP constant for the AuSe and SnS monolayers. (a), (c), (e), and (g) for the elastic modulus. (b), (d), (f), and (h) for the shift of VBM/CBM relative to the vacuum energy under different strains, respectively.

4. Calculational method and results of the Gibbs free energy of HER

The Gibbs free energy is determined by [3–5]:

$$\Delta G_H = \Delta E_H + \Delta E_{ZPE(H)} - T\Delta S_H \quad (7)$$

where ΔE_H denotes the hydrogen binding energy. Here $\Delta E_H = E_{*H} - E_* - 1/2 E_{H_2}$. E_{*H} and E_* are the binding energies of the heterostructure with or without the adsorbed hydrogen atom, respectively. E_{H_2} denotes the binding energy of H_2 molecule in gas. $\Delta E_{ZPE(H)}$ and ΔS_H are the differences in zero-point energies and entropies between the adsorbed H atom and $(1/2)H_2$ in the gas phase, respectively. The contributions from the separate AuSe/SnS heterostructure to both $\Delta E_{ZPE(H)}$ and ΔS_H are small and

negligible. Thus, ΔS_H is approximate -1/2$S_{H_2}^0$, where $S_{H_2}^0$ is the entropy of the gaseous H_2. Under standard conditions, $T\Delta S_H$ is a constant value of 0.2009 eV. $\Delta E_{ZPE(H)}$ can be calculated as $\Delta E_{ZPE(H)} = E_{ZPE(*H)} - E_{ZPE(*)} - 1/2E_{ZPE(H_2)}$, where $E_{ZPE(*H)}$ is the zero-point energy of the AuSe/SnS heterostructure with the adsorbed H atom, $E_{ZPE(*)}$ is the zero-point energy of the separate AuSe/SnS heterostructure, while $E_{ZPE(H_2)}$ is the zero-point energy of H_2 in the gas phase.

Table S11. The adsorption energies of hydrogen molecules on AuSe/SnS heterostructures.

Configuration	Adsorption sites	Adsorption energy(eV)
AS	S6	-2.92
	S9	-2.91
	Se6	-2.73
AxS	S6	-2.91
	S9	-2.92
	Se1	-2.73
AyS	S5	-2.69
	S7	-3.02
	Se2	-2.84

References

[1] C. F. Fu, J. Y. Sun, Q. Q. Luo, X. X. Li, W. Hu and J. L. Yang, *Nano Lett.*,

2018, **18**, 6312–6317.

[2] J. Bardeen and W. Shockley, *Phys. Rev.*, 1950, **80**, 72.

[3] R. Parsons, *Trans. Fara. Soc.*, 1958, **54**, 1053–1063.

[4] C. Ling, L. Shi, Y. Ouyang, X.C. Zeng and J. Wang, *Nano Lett.*, 2017, **17**, 5133–5139.

[5] X. Gao, Y. Zhou, Y. Tan, B. Yang, Z. Cheng, Z. Shen and J. Jia, *Appl. Surf. Sci.*, 2019, **473**, 770–776.